Research Square

Preprints are preliminary reports that have not undergone peer review.
They should not be considered conclusive, used to inform clinical practice,
or referenced by the media as validated information.

A Coupled Geodetic-Atmospheric-Physiological Model of Sustainable Cycling Performance at Altitude

Carlos Alberto Gomez Tarazona

caragomezt@unal.edu.co

Universidad Nacional de Colombia

Carlos E. Guerra-Londoño

Henry Ford Hospital

Daniel R. Izquierdo

University of Applied and Environmental Sciences

Research Article

Keywords:

Posted Date: September 16th, 2026

DOI: https://doi.org/10.21203/rs.3.rs-10912422/v1

License: This work is licensed under a Creative Commons Attribution 4.0 International License.
Read Full License

Additional Declarations: No competing interests reported.

A Coupled Geodetic–Atmospheric–Physiological Model of Sustainable Cycling Performance at Altitude

Carlos G. Tarazona[(a)], Carlos E. Guerra-Londoño[(b,c)], and Daniel R. Izquierdo[(d)]

[(a)] *Department of Physics, Universidad Nacional de Colombia, Bogotá, Colombia.*

[(b)] *Anesthesiologist, Department of Anesthesiology,*
Pain Management, Perioperative Medicine,
Henry Ford Health, Detroit, Michigan, USA.

[(c)] *Clinical Assistant Professor, Michigan State University*
College of Human Medicine, Lansing, Michigan, USA. and

[(d)] *Universidad de Ciencias Aplicadas y Ambientales,*
Facultad de Ciencias, Bogotá, Colombia.

(Dated: September 6, 2026)

Abstract

Cycling performance at altitude reflects a competition between reduced mechanical resistance and altitude-induced physiological impairment. This study develops a coupled geodetic–atmospheric–physiological framework that explicitly distinguishes the mechanical power required by the cyclist–bicycle system from the physiologically available mechanical power. WGS84 normal gravity accounts for altitude- and latitude-dependent geodetic effects, whereas NRLMSIS 2.0 provides atmospheric density with geographic, temporal, seasonal, solar, and geomagnetic dependence. The physiological response is described primarily using the corrected MacInnis meta-regression, with historical altitude-response formulations retained for sensitivity comparison. Sustainable cycling speed is obtained from the equality between required and available mechanical power and optimized over $0 - 4000\,m$. The model confirms that the power required to maintain a fixed speed decreases with altitude. However, under the reference 6% climbing condition, sustainable speed decreases monotonically and no interior optimum is predicted. In contrast, level cycling produces an interior optimum at approximately $2.0 - 2.5\,km$, depending on latitude and atmospheric state. Controlled day-of-year sensitivity calculations show minimal performance differences at the Equator but progressively larger effects at mid and high latitudes, approaching 1% in maximum sustainable speed. These results demonstrate that optimal cycling altitude is not a universal function of elevation or latitude alone, but emerges from the interaction among atmospheric state, road gradient, aerodynamic resistance, and physiological capacity.

I. INTRODUCTION

Cycling performance at altitude results from the interaction of mechanical, atmospheric, geodetic, and physiological mechanisms. From a mechanical perspective, the power required to maintain a given speed is determined by gravitational, rolling-resistance, and aerodynamic forces. Aerodynamic resistance decreases with air density and therefore generally decreases with altitude. Conversely, hypoxic exposure reduces aerobic capacity and sustainable power output. The resulting competition between aerodynamic benefit and physiological impairment has long been recognized as a central determinant of altitude-dependent cycling performance [9, 11, 12].

Previous approaches to altitude-related cycling performance have generally treated these

mechanisms separately or have adopted simplified environmental descriptions. In particular, the International Standard Atmosphere (ISA) provides a useful conventional reference state but does not explicitly represent the observed dependence of atmospheric temperature and density on geographic latitude, season, universal time, and solar and geomagnetic activity. These dependencies can modify atmospheric pressure and density at a given geometric altitude and are therefore relevant when atmospheric effects are incorporated into a quantitative model of cycling performance.

A second environmental contribution arises from the spatial variation of effective gravity. Because terrestrial gravity depends on latitude and altitude, the gravitational component of cycling power is not strictly invariant with geographic location. The WGS84 reference ellipsoid provides a physically consistent framework for describing this dependence.

Physiological performance introduces an additional altitude-dependent limitation. The reduction in maximal aerobic capacity with hypoxia has traditionally been represented using empirical relationships derived from experimental studies. However, these relationships differ according to altitude, exposure duration, acclimatization status, and athlete characteristics. Consequently, a physically based cycling model should distinguish the atmospheric forcing from the physiological response rather than treating altitude as a single empirical performance parameter.

The objective of the present study is therefore to formulate a coupled model of sustainable cycling performance that simultaneously accounts for (i) latitude- and altitude-dependent effective gravity, (ii) geographic- and time-dependent atmospheric density, and (iii) the altitude-dependent reduction in maximal sustainable mechanical power associated with hypoxia. The geodetic component is described using the WGS84 [2] reference ellipsoid, while the atmospheric state is evaluated using the NRLMSIS 2.0 [3] empirical atmospheric model, with the International Standard Atmosphere (ISA) [5] retained as a conventional reference atmosphere. This formulation allows the effect of latitude and atmospheric conditions to be separated from the purely altitude-dependent effects traditionally represented by standard-atmosphere models.

The resulting framework is used to determine how the coupling between the altitude-induced reduction in required mechanical power and the decline in physiologically available power affects the maximum sustainable cycling speed and its dependence on altitude and latitude.

To analyze steady cycling at a prescribed altitude, the climb is represented by its mean road gradient. At each prescribed environmental state, acceleration is assumed to be zero and the corresponding cycling speed is locally constant. This steady-state assumption does not imply that the same sustainable speed is maintained at different altitudes. In the coupled model developed below, v_{sus} is independently determined at each altitude and latitude. Under these conditions, the force balance along the normal and tangential directions can be written as

$$\begin{aligned} \sum F_y &= N - m_S g\,(h,\phi)\cos\theta = 0, \\ \sum F_x &= F_{cyc} - m_S g\,(h,\phi)\sin\theta - F_{roll} - F_D = 0, \end{aligned} \tag{1}$$

where N is the normal force exerted by the road, $m_S = m_c + m_b$ is the total cyclist–bicycle system mass, with m_c and m_b denoting cyclist and bicycle mass, respectively, $g\,(h,\phi)$ is the WGS84 normal gravity, θ is the road inclination angle, F_{cyc} is the propulsive force, F_{roll} is the rolling-resistance force, which depends on the normal force from the road and the rolling coefficient c_r (this dimensionless coefficient depends on the tire casing, the rubber compound, the pressure, and the paved surface), where

$$F_{roll} = c_r N \tag{2}$$

and F_D is the aerodynamic drag force. This last term deserves special attention. At sufficiently high cycling speeds, aerodynamic drag can represent a major fraction of the mechanical power required to maintain a prescribed velocity [1, 24, 25]. The aerodynamic resistance is represented by the conventional quadratic drag relation

$$F_D = \frac{1}{2}\rho C_d A v^2 \tag{3}$$

where ρ is the atmospheric mass density and C_dA is the aerodynamic drag area of the cyclist–bicycle system. The drag area incorporates both the dimensionless drag coefficient and the projected frontal area and is the parameter directly determining aerodynamic resistance [24, 25]. For the present theoretical analysis, C_dA is assumed constant for a prescribed cycling position. Variations caused by changes in cyclist posture are therefore outside the scope of the primary model. Wind is neglected, so that the relative air speed is taken to be equal to the ground speed, $v_{air} = v$.

Substituting Equations (2) and (3) into the tangential force balance in Equation (1) gives

$$F_{cyc} - m_S g\,(h,\phi)\sin\theta - c_r m_S g\,(h,\phi)\cos\theta - \frac{1}{2}\rho C_d A v^2 = 0. \tag{4}$$

Mechanical power is defined as the scalar product of force and velocity, $P = \vec{F}\cdot\vec{v}$. Multiplying the tangential force balance in Equation (4) by the cycling speed therefore gives the required external mechanical power

$$P_{req} = \frac{1}{2}\rho C_d A v^3 + m_S g\,(h,\phi)\,(\sin\theta + c_r\cos\theta)\,v \tag{5}$$

In this formulation, $P_{req} = F_{cyc}v$ represents the external mechanical power required to overcome aerodynamic, gravitational, and rolling-resistance forces. Direct comparison with crank-based power-meter measurements would additionally require consistent treatment of drivetrain and bearing losses [1]. Mechanical models of cycling and physiological models of altitude-induced performance decline have traditionally been developed separately [1, 8, 18]. The present framework couples these contributions by distinguishing the mechanical power required by the external resistive forces, P_{req}, from the physiologically available mechanical power, P_{avail}.

II. VARIATION OF GRAVITY AND AIR DENSITY WITH ALTITUDE

The effective weight of the cyclist–bicycle system depends on the local normal gravity, which varies with geodetic latitude and altitude. Within WGS84, normal gravity incorporates both Earth's oblateness and rotation and may be written as

$$W\,(h,\phi) = m_S\, g\,(h,\phi)$$

where $g\,(h,\phi)$ is the normal gravity at geometric altitude h above the WGS84 reference ellipsoid (measured along the geodetic vertical) and at a geodetic latitude ϕ. The WGS84 normal-gravity field incorporates both gravitational attraction and the centrifugal effect of Earth's rotation while accounting for terrestrial oblateness. At the reference ellipsoid ($h = 0$) normal gravity is given by [2, 4]

$$g_0\,(\phi) = 9.7803253359\frac{1 + 0.00193185265241\sin^2\phi}{\sqrt{1 - 0.00669437999013\sin^2\phi}}\left[m\cdot s^{-2}\right], \tag{6}$$

The variation in normal gravity can be quantified by comparing its value at the equator ($\phi = 0$), where $g_0\,(0) = 9.7803253359\,m\cdot s^{-2}$, and at the poles ($\phi = 90°$) where we obtain

$g_0(90°) = 9.8321849378\, m \cdot s^{-2}$ and for reference, at ($\phi \approx 45°$), $g_0(45°) = 9.8061977694\, m \cdot s^{-2}$. Considering a point at a height h, normal gravity above the WGS84 ellipsoid is represented by the second-order Taylor expansion [6, 7]

$$g(h,\phi) = g_0(\phi)\left[1 - \frac{2}{a}\left(1 + f + m_\omega - 2f\sin^2\phi\right)h + \frac{3}{a^2}h^2\right] \tag{7}$$

where $a = 6378137.0$ is the value of the semi-major axis of the ellipsoid, $f = 1/298.257223563$ is the flattening, $m_\omega = \frac{\omega^2 a^2 b}{G\, m_\oplus} \approx 0.003449786003$ is the ratio of centrifugal to gravitational effects at the equator [2, 4]. The gravitational attraction of atmospheric mass is neglected because its contribution is negligible over the $(0 - 4000)\, m$ altitude range considered here.

The weight as a function of height will be

$$W(h,\phi) = m_S g(h,\phi) = m_S g_0(\phi)\left[1 - A_g(\phi)\, h + B_g h^2\right] \tag{8}$$

where we have defined

$$\begin{aligned} A_g(\phi) &= \tfrac{2}{a}\left(1 + f + m_\omega - 2f\sin^2\phi\right) \\ B_g &= \tfrac{3}{a^2}. \end{aligned} \tag{9}$$

Although these variations are small in relative magnitude, they enter explicitly into the gravitational and rolling-resistance terms of the mechanical power model and therefore provide a systematic latitude-dependent correction.

Throughout the mechanical model, h denotes geometric altitude above the reference ellipsoid unless otherwise specified. NRLMSIS 2.0 internally uses geopotential height as its vertical coordinate; the model output is therefore evaluated using its prescribed altitude conversion.

Variation of air density with altitude

For reference, under hydrostatic equilibrium and an isothermal ideal-gas approximation, atmospheric pressure and density satisfy

$$\frac{dP}{dh} = -\rho g \tag{10}$$

where ρ is the density of air. From the ideal gas equation, we have that

$$\rho = \frac{PM}{RT} \tag{11}$$

where R is the universal gas constant $\left(8.314 J \cdot (mol \cdot K)^{-1}\right)$, M is the molar mass of dry air ($\approx 0.02896\, kg \cdot mol^{-1}$), and T is the atmospheric temperature. If T and g are treated as locally constant, Equation (10) becomes

$$\frac{dP}{P} = -\frac{Mg}{RT}dh \tag{12}$$

Integration of Equation (12) gives the familiar barometric relation

$$\rho\left(h\right) = \rho_0 e^{-\frac{h}{H}} \tag{13}$$

where $\rho_0 \approx 1.225\, kg \cdot m^{-3}$ is the ISA sea-level reference density corresponding to $T = 288.15\, K$ and a pressure of one atmosphere $1atm = 101325\, Pa$, and H is defined as the scale height, given by the relationship

$$H = \frac{RT}{Mg}. \tag{14}$$

This isothermal formulation is not used as the final atmospheric specification because it neglects the observed dependence of atmospheric state variables on geographic and temporal conditions. For the altitude range considered here, $0 \leq h \leq 4\, km$, the relevant ISA layer is the troposphere, in which temperature is approximated by

$$T\left(h\right) = T_0 - Lh \tag{15}$$

with $T_0 = 288.15\, K$ and $L = 0.0065\, K \cdot m^{-1}$. Substituting the WGS84 gravity approximation of Equation (7) and the tropospheric temperature profile of Equation (15) into Equation (12) gives

$$\frac{dP}{P} = -\frac{Mg\left(h,\phi\right)}{RT\left(h\right)}dh = -\frac{Mg_0\left(\phi\right)}{R}\frac{1 - A_g\left(\phi\right)h + B_g h^2}{T_0 - Lh}dh \tag{16}$$

or equivalently

$$\frac{dP}{P} = -\frac{Mg_0\left(\phi\right)}{R}\frac{dh}{T_0 - Lh} + \frac{Mg_0\left(\phi\right)}{R}\frac{A_g\left(\phi\right)h - B_g h^2}{T_0 - Lh}dh \tag{17}$$

Over the altitude range considered here, the altitude-dependent corrections to WGS84 normal gravity remain small. The largest value of $A_g\left(\phi\right)$ occurs near the equator and is approximately $3.1577 \times 10^{-7} m^{-1}$, for $h = 4000\, m$, $A_g\left(\phi\right)h \approx 0.0012$, corresponding to a contribution of only 0.12%, whereas $B_g \approx 7.3745 \times 10^{-14} m^{-2}$ is $B_g h^2 \approx 1.1799 \times 10^{-6}$ corresponding to a contribution of only 1.1799×10^{-4}%. Therefore, the contribution of the second term of the equation (17) is very small and we can neglect it. Integrating only the first term and using

the ideal gas Equation (11), we obtain

$$\rho_{ISA-m}(h,\phi) = \rho_0 \left(1 - \frac{Lh}{T_0}\right)^{\frac{Mg_0(\phi)}{RL}-1} \tag{18}$$

Equation (18) defines a modified standard-atmosphere formulation, hereafter denoted $\rho_{ISA-m}(h,\phi)$, in which the conventional tropospheric temperature lapse-rate model is retained while the constant standard gravitational acceleration is replaced by the latitude-dependent WGS84 surface normal gravity $g_0(\phi)$. The altitude-dependent gravity corrections $A_g(\phi)\,h$ and $B_g h^2$ remain smaller than approximately 0.12% over the $(0-4000)\,m$ altitude range and are neglected in this closed-form approximation. ISA-m is introduced only as an analytical sensitivity model to isolate the geodetic contribution of latitude. It should not be interpreted as the official ISA or as a representation of actual local atmospheric conditions. All primary atmospheric calculations presented in the Results are performed using NRLMSIS 2.0.

Atmospheric specification using NRLMSIS 2.0

The limitations of an altitude-only standard atmosphere motivate the use of the NRLMSIS 2.0 [3] empirical atmospheric model. Unlike the ISA formulation, NRLMSIS 2.0 represents the atmospheric state as a function of altitude, geographic location, time, solar activity, and geomagnetic activity. The model directly provides atmospheric temperature, neutral-species densities, and total neutral mass density. NRLMSIS 2.0 uses geopotential height as its internal vertical coordinate and calculates geopotential height from geodetic altitude and latitude using the WGS84 reference ellipsoid and associated gravitational field. In the present cycling model, however, the WGS84 normal-gravity formulation is retained explicitly in the mechanical power equation so that the gravitational contribution to cycling power can be evaluated independently of the atmospheric model.

For the present cycling application, NRLMSIS 2.0 is evaluated at the geographic latitude and longitude of the location under consideration, for the specified date and universal time, together with the corresponding solar and geomagnetic activity indices. The resulting atmospheric temperature and neutral atmospheric mass density are then used directly in the aerodynamic term of the cycling-power equation. For the present aerodynamic formulation, this neutral atmospheric mass density is used as the air-density input in the aerodynamic

drag term. Consequently, atmospheric temperature and density at a prescribed geodetic altitude may vary with latitude, longitude, day of year, universal time, and the specified solar and geomagnetic forcing.

For the primary NRLMSIS 2.0 calculations, atmospheric temperature is obtained directly from the empirical model rather than from the linear lapse-rate relation used in ISA-m. We therefore denote the NRLMSIS 2.0 temperature output as

$$T_{atm} = T_{NRLMSIS}\left(h, \phi, \lambda, t, d, F_{10.7}, F_{10.7A}, A_p\right) \tag{19}$$

Here h is the geodetic altitude supplied to the NRLMSIS 2.0 implementation; internally, the model converts this quantity to geopotential height, ϕ is geodetic latitude, λ is geographic longitude, t is the time specification used by pymsis/NRLMSIS, d is the day of year, $F_{10.7}$ is the daily solar radio flux, $F_{10.7A}$ is its centered 81-day running mean and A_p denotes the seven geomagnetic indices corresponding to the storm-time scheme. The precise values used in each numerical experiment are reported in Section IV to ensure reproducibility.

Here T_{atm} denotes the temperature returned by the empirical model for the specified input state; it is not an analytical temperature law derived in the present work. In fact, NRLMSIS 2.0 provides atmospheric temperature as part of its state description, but only the neutral mass density enters directly into the aerodynamic power term used in the present mechanical model.

Equation (18) is retained as the analytical ISA-m sensitivity model. For the primary atmospheric calculations, however, the neutral atmospheric mass density is obtained directly from NRLMSIS 2.0 as

$$\rho_{atm} = \rho_{NRLMSIS}\left(h, \phi, \lambda, t, d, F_{10.7}, F_{10.7A}, A_p\right) \tag{20}$$

the Equation (20) represents a model output rather than an analytical density law. Because NRLMSIS 2.0 directly provides the neutral atmospheric mass density required by the aerodynamic drag formulation, no additional hydrostatic integration is required for the NRLMSIS-based calculations.

Although NRLMSIS 2.0 internally accounts for the gravitational field through its geopotential-height formulation, the present study retains the explicit WGS84 gravity formulation in the cycling mechanical model so that the direct contribution of gravity to the required cycling power can be quantified separately.

NRLMSIS 2.0 should be interpreted here as an empirical atmospheric reference model rather than as a local weather forecast or a high-resolution meteorological analysis.

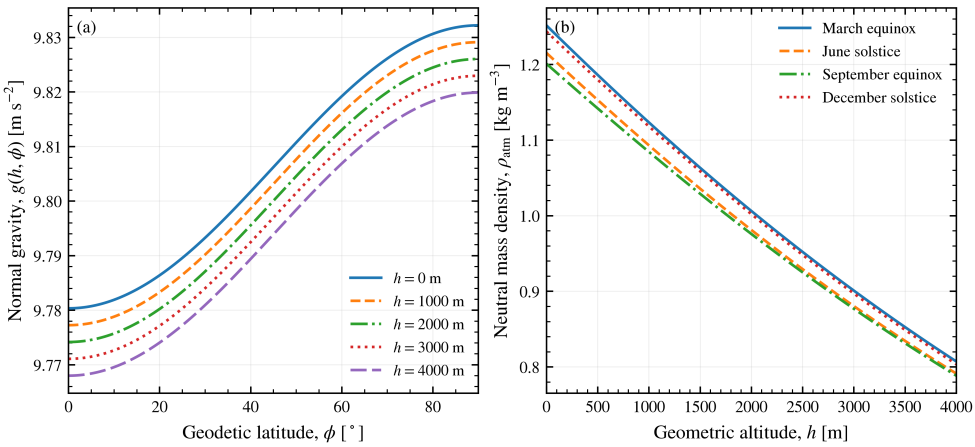


FIG. 1. Geodetic and atmospheric dependence of the environmental quantities entering the cycling model. (a) WGS84 normal gravity $g\,(h, \phi)$ as a function of geodetic latitude for selected geometric altitudes between 0 and 4000 m. Normal gravity increases systematically with latitude and decreases with altitude. (b) NRLMSIS 2.0 neutral atmospheric mass density as a function of geometric altitude at $\phi = 45°$ for representative dates near the March equinox, June solstice, September equinox, and December solstice. Longitude, Universal Time, $F_{10.7}$, $F_{10.7A}$, and geomagnetic activity were held fixed in panel (b), so that the comparison isolates the day-of-year dependence of the atmospheric model rather than representing a climatological forecast.

Figure 1 demonstrates that the environmental state entering the cycling model cannot be represented by geometric altitude alone. The geodetic contribution depends explicitly on latitude through $g\,(h, \phi)$, whereas the atmospheric contribution depends additionally on geographic location, day of year, time, and solar and geomagnetic forcing through ρ_{atm}. These two contributions are propagated independently into the mechanical power model developed below.

Mechanical power during climbing

Combining the mechanical formulation of Equation (5) with the WGS84 gravity field and the NRLMSIS 2.0 atmospheric density gives

$$P_{req} = P_{aero} + P_{grav} + P_{roll} \tag{21}$$

where

$$P_{aero} = \tfrac{1}{2}\rho_{atm} C_d A v^3,$$
$$P_{grav} = m_S g\,(h, \phi) \sin\theta\, v,$$
$$P_{roll} = m_S g\,(h, \phi)\, c_r \cos\theta\, v$$

For a prescribed cycling speed, the altitude derivative of the total required mechanical power is obtained directly from Equation (21)

$$\left(\frac{\partial P_{req}}{\partial h}\right)_{v,\phi} = \frac{1}{2} C_d A v^3 \left(\frac{\partial \rho_{atm}}{\partial h}\right)_{\phi} + m_S v\,(\sin\theta + c_r \cos\theta) \left(\frac{\partial g\,(h, \phi)}{\partial h}\right)_{\phi}.$$

Because both atmospheric density and normal gravity decrease over the altitude range considered, the derivative is negative for fixed cycling speed, road gradient, and aerodynamic configuration:

$$\left(\frac{\partial P_{req}}{\partial h}\right)_{v,\phi} < 0 \tag{22}$$

Thus, the total mechanical power required to maintain a prescribed speed decreases with altitude.

Unless otherwise stated, all numerical calculations are performed over the geometric-altitude interval $0 \leq h \leq 4000\,m$. The WGS84 gravity model is evaluated at geometric altitude, whereas NRLMSIS 2.0 performs its internal vertical calculations using geopotential height.

For subsequent coupling with the physiological model, it is useful to make the complete dependence of the required mechanical power explicit. Equation (21) can therefore be written in functional form as

$$P_{req} = P_{req}\,(h, \phi, \lambda, t, d, F_{10.7}, F_{10.7A}, A_p, v, \theta, m_s, C_d A, c_r)$$

Latitude enters the mechanical demand through two independent pathways: directly through the WGS84 normal gravity $g\,(h, \phi)$, and indirectly through the geographic dependence of the NRLMSIS 2.0 atmospheric density. In the fixed-speed mechanical analysis v is prescribed. In the coupled performance model developed in Section III, by contrast, the sustainable speed v_{sus} becomes the dependent variable determined from the equality between required and physiologically available mechanical power.

III. PHYSIOLOGICAL POWER AVAILABILITY AND COUPLING WITH CYCLING MECHANICS

The principal acute physiological consequence of increasing altitude is the reduction in inspired oxygen partial pressure caused by decreasing barometric pressure. This reduces alveolar and arterial oxygen partial pressures and arterial oxygen saturation, thereby constraining oxygen delivery during maximal exercise [8, 10, 15, 23]. The resulting decrease in maximal oxygen uptake, $\dot{V}O_{2\,\max}$, represents an important limitation of aerobic performance, although it should not be interpreted as identical to sustainable mechanical cycling power.

Wehrlin and Hallén [8] studied endurance-trained athletes during acute exposure to simulated altitudes of $300, 800, 1300, 1800, 2300$, and $2800\,m$. $\dot{V}O_{2\,\max}$ declined approximately linearly over this range, corresponding to an average reduction of 6.3% per $1000\,m$, and both $\dot{V}O_{2\,\max}$ and performance were already significantly reduced between 300 and $800\,m$. Thus, the available experimental evidence does not support imposing a sharp physiological threshold at $1500\,m$.

For prolonged cycling, the relationship between maximal aerobic capacity and sustainable mechanical power is task dependent. Critical power, fractional utilization of $\dot{V}O_{2\,\max}$, and cycling economy may all modify the translation of aerobic capacity into external mechanical power. For example, Oberholzer et al. [16] reported reductions of $11.2\pm3.0\%$ in $\dot{V}O_{2peak}$ and $10.7\pm3.1\%$ in mean power during a 40-min cycling time trial at $2800\,m$ compared with $300\,m$, together with increased fractional utilization and poorer cycling economy. Accordingly, the proportional scaling adopted below is treated explicitly as a modeling approximation rather than as a universal physiological law.

Cycling-specific evidence is provided by Townsend et al. [13], who determined CP and W' in nine trained cyclists during acute hypoxic exposure at $250, 1250, 2250, 3250$, and $4250\,m$. CP decreased significantly with increasing altitude and was described by a third-order polynomial relationship ($R^2 = 0.99$), whereas W' showed a significant reduction only at $4250\,m$. These results demonstrate that sustainable cycling power is altitude dependent and provide an important independent validation of the physiological penalty considered in the present model. However, because the Townsend relationship was obtained from a relatively small sample under acute hypoxia and was developed specifically for CP/W' modeling, it is

used here as an independent physiological comparison rather than as the primary altitude-response model.

At a broader performance level, Deb et al. [22] conducted a systematic review and meta-regression of acute hypoxic exposure including 82 outcomes from 53 studies and 798 participants. Their analysis confirmed a progressive ergolytic effect of increasing hypoxic dose on exercise performance and capacity, with nonlinear responses for time-trial and time-to-exhaustion exercise. These findings further support the use of a nonlinear physiological response to altitude, although the Deb et al. model is not used directly as the physiological scaling function in the present work.

Let τ denote the prescribed duration of the modeled effort, and let $P_0(\tau)$ denote the sustainable mechanical power available from the cyclist at sea level for that duration and let $V_0 = \dot{V}O_{2\max}(0)$ denote the corresponding baseline maximal oxygen uptake. The association between aerobic capacity and cycling power is well established in trained cyclists [14]. Nevertheless, sustainable mechanical power is not determined by $\dot{V}O_{2\max}$ alone. The present model therefore adopts the more limited assumption that the relative altitude-induced change in sustainable mechanical-power availability scales approximately with the relative change in maximal aerobic capacity. Accordingly,

$$\frac{P_{avail}(h, V_0, \tau)}{P_0(\tau)} \approx \frac{\dot{V}O_{2\max}(h, V_0)}{V_0} = F_{phys}(h, V_0) \tag{23}$$

The effort duration τ is fixed within each numerical experiment; its effect is therefore contained in the reference value $P_0(\tau)$, whereas the altitude scaling is described by F_{phys}. Equation (23) is an explicit modeling assumption and should not be interpreted as an identity between $\dot{V}O_{2\max}$ and sustainable cycling power.

The primary contemporary physiological formulation adopted here is the meta-regression developed by MacInnis et al. [19] and corrected in the subsequently published corrigendum [20] . The analysis was based on 105 independent participant groups comprising 958 subjects from 80 studies and demonstrated interacting and curvilinear effects of altitude and baseline $\dot{V}O_{2\max}$ on the response to acute hypoxia.

The MacInnis meta-regression describes acute hypoxic exposure and is therefore adopted as the primary contemporary physiological model for the present analysis. Acclimatization is not implicitly assumed in this formulation.

$$\widehat{\Delta V}_{MI}(z, V_0) = 5.5913\left(-7.7328 + 1.1872z + 0.2940V_0 - 0.0777z^2 - 0.0027V_0^2 - 0.0283zV_0\right) \tag{24}$$

Here $\widehat{\Delta V}_{MI}$ denotes the signed meta-regression prediction of the altitude-induced change in $\dot{V}O_{2\max}$, expressed in $mL \cdot (kg \cdot min)^{-1}$, V_0 is expressed in the same units and we define $z = \frac{h}{1000\,m}$ and use z as the numerical altitude in kilometres throughout the physiological regressions.

The original meta-regression was not constrained to yield exactly zero change at zero altitude. Because the coupled cycling framework requires the physiological scaling factor to satisfy $F_{phys}(0, V_0) = 1$, we introduce a sea-level anchoring of the MacInnis prediction

$$\dot{V}O^{MI}_{2\max}(h, V_0) = V_0 + \widehat{\Delta V}_{MI}(z, V_0) - \widehat{\Delta V}_{MI}(0, V_0) \tag{25}$$

Substitution of Equation (24) into the sea-level normalization in Equation (25) cancels all altitude-independent terms. This anchoring is introduced in the present work and is not part of the original MacInnis formulation. It yields the following explicit physiological scaling factor:

$$F_{MI}(h, V_0) = \frac{\dot{V}O^{MI}_{2\max}}{V_0} = 1 + \frac{5.5913}{V_0}\left[(1.1872 - 0.0283V_0)\,z - 0.0777z^2\right] \tag{26}$$

Equation (26) is therefore used as the primary physiological scaling function. It satisfies $F_{MI}(0, V_0) = 1$ by construction and retains both the nonlinear altitude dependence and the interaction with baseline aerobic capacity contained in the MacInnis meta-regression.

For historical comparison, the empirical altitude-response relationships used by Bassett et al. [27], based on the earlier synthesis of Howley [28], are retained as sensitivity models. These formulations distinguish between acute/unacclimatized and acclimatized responses and are not used in the primary physiological calculations.

$$F_{HB,U}(z) = \frac{0.178z^3 - 1.43z^2 - 4.07z + 100}{100} \tag{27}$$

where z denotes the numerical altitude expressed in kilometres and the subscript U denotes the historical unacclimatized formulation. The cubic form captures the stronger nonlinear impairment historically assigned to acute, unacclimatized exposure.

For acclimatized subjects, the model is given by

$$F_{HB,A}(z) = \frac{-1.12z^2 - 1.90z + 99.9}{99.9} \tag{28}$$

The subscript A denotes the historical acclimatized formulation. This relationship predicts an increasingly steep physiological decline with altitude. These historical relationships (27 and 28) are not used as the primary physiological model.

Péronnet et al. [17, 18] developed an independent theoretical treatment of altitude-dependent endurance performance, including a physiological description related to barometric pressure. Accordingly, Equations (27) and (28) are identified here as historical Howley–Bassett formulations and are not attributed to Péronnet.

Recent work has revisited the interaction between aerodynamic benefit and physiological impairment in altitude cycling. Vinetti [26], discussing the cycling hour record, contrasted contemporary altitude-response approaches with earlier cycling models and explicitly considered the relevance of the MacInnis meta-regression together with the historical Bassett formulation. This motivates the use of the MacInnis relationship as the primary contemporary physiological model in the present study while retaining older relationships only for sensitivity analysis.

Complementary empirical evidence is provided by Harnish et al. [21], who analyzed more than 600 cycling hour records and reported a small but statistically significant marginal benefit of elevation up to approximately $1000\,m$, followed by declining performance at higher elevations. Because hour-record cycling is essentially level and strongly dominated by aerodynamic resistance, these observations are used here as contextual evidence for the existence of an altitude-dependent optimum rather than as direct validation of the climbing model.

Using the primary physiological scaling factor, the altitude-dependent sustainable mechanical power available from the cyclist is

$$P_{avail}\left(h, V_0, \tau\right) = P_0\left(\tau\right) F_{MI}\left(h, V_0\right) \tag{29}$$

By definition, $P_{avail}\left(0, V_0, \tau\right) = P_0\left(\tau\right)$. The physiological model therefore determines the power available from the cyclist, whereas Equation (21) independently determines the mechanical power required by the cyclist–bicycle system.

At a given altitude and latitude, the maximum sustainable cycling speed v_{sus} is determined by equality between required and available mechanical power

$$P_{req}\left(h, \phi, \lambda, t, d, F_{10.7}, F_{10.7A}, A_p, v_{sus}, \theta, m_s, C_dA, c_r\right) = P_{avail}\left(h, V_0, \tau\right)$$

Substituting Equation (21) into the power-balance condition gives

$$\frac{1}{2}\rho_{atm} C_d A v_{sus}^3 + m_S g\left(h,\phi\right)\sin\theta\, v_{sus} + m_S g\left(h,\phi\right) c_r \cos\theta\, v_{sus} = P_0\left(\tau\right) F_{MI}\left(h, V_0\right) \tag{30}$$

For a prescribed latitude and a fixed set of atmospheric, biomechanical, and physiological parameters, the constrained optimal altitude is defined as

$$h_{opt}\left(\phi,\gamma\right) = \underset{0\le h\le 4000\,m}{\arg\max}\; v_{sus}\left(h,\phi,\gamma\right) \tag{31}$$

with

$$\gamma = \{\lambda, t, d, F_{10.7}, F_{10.7A}, A_p, V_0, P_0\left(\tau\right), \tau, \theta, m_s, C_d A, c_r\} \tag{32}$$

Equation (31) defines the constrained optimal altitude h_{opt}. When the optimum lies strictly inside the prescribed altitude interval, it is denoted by h_c and satisfies the stationary and second-derivative conditions derived below. If the maximum occurs at either boundary, no interior critical altitude exists. The parameter set γ contains the atmospheric, biomechanical, and physiological quantities held fixed during a latitude-sensitivity calculation. The sustainable speed v_{sus} is not included in γ because it is the dependent variable determined from Equation (30).

For an interior optimum, the critical-altitude condition follows from implicit differentiation of the sustainable-power balance. For a prescribed latitude ϕ and γ, the sustainable speed $v_{sus}\left(h,\phi\right)$ is implicitly defined by

$$B\left(h,\phi,v_{sus},\gamma\right) = P_{req}\left(h,\phi,v_{sus},\gamma\right) - P_{avail}\left(h,V_0,\tau\right) = 0 \tag{33}$$

Differentiation with respect to altitude gives

$$\left(\frac{\partial P_{req}}{\partial h}\right)_{v_{sus}} + \frac{\partial P_{req}}{\partial v_{sus}}\frac{dv_{sus}}{dh} - \frac{dP_{avail}}{dh} = 0 \tag{34}$$

Therefore,

$$\frac{dv_{sus}}{dh} = \frac{\frac{dP_{avail}}{dh} - \left(\frac{\partial P_{req}}{\partial h}\right)_{v_{sus}}}{\frac{\partial P_{req}}{\partial v_{sus}}} \tag{35}$$

where

$$\frac{\partial P_{req}}{\partial v_{sus}} = \frac{3}{2}\rho_{atm} C_d A v_{sus}^2 + m_S g\left(h,\phi\right)\left(\sin\theta + c_r\cos\theta\right) > 0$$

At an interior maximum of sustainable cycling speed, $\frac{dv_{sus}}{dh} = 0$. Since the denominator in Equation (35) is strictly positive for the physical parameter range considered, the interior critical altitude satisfies

$$\left(\frac{\partial P_{req}}{\partial h}\right)_{v_{sus}}\Bigg|_{h_c,\phi,v_c} = \left.\frac{\partial P_{avail}}{\partial h}\right|_{h_c} \tag{36}$$

where $v_c = v_{sus}\left(h_c, \phi\right)$. The derivative of P_{req} appearing in Equation (36) is a partial derivative with respect to altitude at fixed cycling speed, not the total derivative evaluated along the sustainable-speed solution curve.

Substituting Equation (21) into Equation (36) gives

$$\frac{1}{2}C_d A v_c^3 \left.\frac{\partial \rho_{atm}}{\partial h}\right|_{h_c,\phi} + m_S v_c \left(\sin\theta + c_r\cos\theta\right) \left.\frac{\partial g\left(h,\phi\right)}{\partial h}\right|_{h_c,\phi} = P_0\left(\tau\right) \left.\frac{\partial F_{MI}\left(h, V_0\right)}{\partial h}\right|_{h=h_c} \tag{37}$$

Differentiation of Equation (26) gives

$$\frac{\partial F_{MI}\left(h, V_0\right)}{\partial h} = \frac{5.5913}{1000 V_0}\left(1.1872 - 0.0283 V_0 - 0.1554 z\right) \tag{38}$$

Equation (37) is the explicit geodetic–atmospheric–physiological equilibrium condition of the present model. The left-hand side represents the altitude-induced reduction in required mechanical power, including both the NRLMSIS 2.0 density contribution and the WGS84 gravity contribution. The right-hand side represents the altitude-induced reduction in physiologically available mechanical power predicted from the contemporary MacInnis scaling model.

For the baseline aerobic-capacity range considered in the present study $50 - 70\, mL \cdot kg^{-1} \cdot min^{-1}$ and for the atmospheric profiles evaluated here, the three altitude derivatives appearing in Equation (37) are negative. Equation (37) may therefore be interpreted as an equality between the magnitude of the altitude-induced mechanical benefit and that of the physiological penalty.

It is important to note

$$\left.\frac{d^2 v_{sus}}{dh^2}\right|_{h=h_c} < 0 \tag{39}$$

Equation (39) distinguishes an interior maximum of sustainable cycling speed from any other stationary solution. If no interior point simultaneously satisfies Equations (36) and (39) over the prescribed altitude interval, the constrained optimum occurs at one of the interval boundaries.

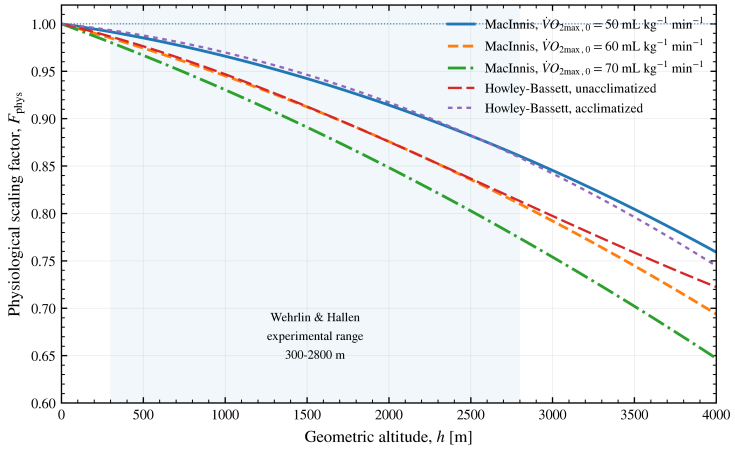


FIG. 2. Contemporary and historical physiological scaling factors as functions of geometric altitude. MacInnis-based curves are shown for baseline $\dot{V}O_{2\,\max}$ values of $50, 60$, and $70\,mL \cdot kg^{-1} \cdot min^{-1}$, whereas the historical unacclimatized and acclimatized Howley–Bassett formulations are included for sensitivity comparison. The shaded region indicates the $300 - 2800\,m$ experimental range investigated by Wehrlin and Hallén and does not represent an uncertainty interval. The corrected MacInnis formulation is used as the primary physiological model in the subsequent calculations.

It should be emphasized that the MacInnis meta-regression describes acute hypoxic exposure. Consequently, the primary MacInnis predictions shown in Figure 2 should not be interpreted as an acclimatized response. The historical acclimatized Howley–Bassett curve is retained only as a sensitivity scenario. At $2800\,m$, the historical unacclimatized and acclimatized factors are approximately 0.813 and 0.859, respectively. These values differ substantially from the MacInnis prediction for highly aerobically trained individuals, illustrating that the predicted physiological penalty and therefore the coupled altitude response depends on both the physiological formulation and baseline aerobic capacity.

Interestingly, for a baseline $\dot{V}O_{2\,\max}$ of $70\,mL \cdot kg^{-1} \cdot min^{-1}$, the initial slope of the normalized MacInnis model is approximately -6.34% per $1000\,m$, closely matching the mean 6.3% per $1000\,m$ decline reported experimentally by Wehrlin and Hallén in endurance-trained athletes.

IV. NUMERICAL IMPLEMENTATION AND RESULTS

The coupled model was evaluated over the geometric-altitude interval $0 \leq h \leq 4000\,m$. Atmospheric temperature and neutral mass density were obtained using NRLMSIS 2.0, whereas normal gravity was calculated independently from the WGS84 formulation introduced in Section II. To isolate the effect of latitude, all atmospheric inputs other than geodetic latitude were held fixed within each latitude-sensitivity experiment. Three representative latitudes, $\phi = 0°, 45°$ and $71°$, were considered to sample equatorial, mid-latitude, and high-latitude conditions, respectively. These values are used as idealized latitude cases and are not intended to reproduce the complete meteorological state of specific cycling races.

For each altitude and latitude, the NRLMSIS 2.0 neutral mass density was inserted into Equation (30), together with the corresponding WGS84 normal gravity. The sustainable cycling speed v_{sus} was then obtained as the unique positive solution of the mechanical–physiological power-balance equation. The contemporary MacInnis formulation was used for the primary physiological calculations, whereas the Howley–Bassett relationships were retained only for sensitivity analyses.

For numerical purposes, Equation (30) may be written as

$$f\left(v_{sus}\right) = a v_{sus}^{3} + b v_{sus} - P_{avail}\left(h, V_0, \tau\right) = 0 \tag{40}$$

where

$$\begin{aligned} a\left(h,\phi\right) &= \tfrac{1}{2}\rho_{atm} C_d A \\ b\left(h,\phi\right) &= m_S g\left(h,\phi\right)\left(\sin\theta + c_r \cos\theta\right) \end{aligned}$$

For physically admissible parameters, $a > 0, b > 0$, and $P_{avail} > 0$. Moreover

$$\frac{\partial f}{\partial v_{sus}} = 3a\left(h,\phi\right) v_{sus}^{2} + b\left(h,\phi\right) > 0\,;\; v_{sus} > 0 \tag{41}$$

Thus, $f\left(v_{sus}\right)$ is strictly increasing for positive cycling speed. Since $f\left(0\right) = -P_{avail} < 0$ and $f\left(v_{sus}\right) \to +\infty$ as $v_{sus} \to \infty$, Equation (40) has exactly one positive physically admissible solution at every altitude.

Aerodynamic resistance is parameterized directly through the drag area $C_d A$, rather than by prescribing C_d and A independently. This choice follows standard cycling-aerodynamics practice because $C_d A$ directly determines aerodynamic power and avoids the additional uncertainty associated with separating drag coefficient and projected frontal area [24, 25].

Wind-tunnel data summarized by Crouch et al. [25] report drag-area values of approximately $0.26 - 0.29\,m^2$ for compact road-cycling positions and values extending to approximately $0.28 - 0.36\,m^2$ for more upright configurations. Martin et al. [1] reported an average drag area of approximately $0.2642\,m^2$ for cyclists adopting relatively aerodynamic positions. Accordingly, $C_dA = 0.30\,m^2$ was selected as the reference value for the present road-cycling model. Values of 0.26 and $0.35\,m^2$ were additionally evaluated to quantify the sensitivity of the predicted optimal altitude to aerodynamic configuration.

The coefficient of rolling resistance was set to $c_r = 0.0032$. Martin et al. [1] adopted this value as the mean of experimentally reported coefficients ranging from approximately 0.0027 to 0.0040 for high-pressure road bicycle tires on smooth asphalt. Accordingly, $c_r = 0.0032$ was used in the reference calculation, whereas the interval $0.0027 \leq c_r \leq 0.0040$ was retained for mechanical sensitivity analyses.

The primary physiological reference scenario corresponds to a 40-min effort with $V_0 = 60\,mL \cdot kg^{-1} \cdot min^{-1}$. These values closely match the cohort studied by Oberholzer et al. [16], which comprised sixteen lowlanders with a mean body mass of $68 \pm 8\,kg$ and a baseline $\dot{V}O_{2peak}$ of $60 \pm 8\,mL \cdot kg^{-1} \cdot min^{-1}$. Accordingly, the reference cyclist mass was set to $m_c = 68\,kg$. Baseline values of $V_0 = 50$ and $70\,mL \cdot kg^{-1} \cdot min^{-1}$ were retained for physiological sensitivity analyses.

A bicycle mass of $m_b = 10\,kg$ was adopted following the representative road-cycling calculation of Martin et al. [1], giving a reference system mass $m_S = 78\,kg$. System masses of 70 and $86\,kg$ were additionally considered in the sensitivity analysis.

In the experimental protocol preceding the final study of Oberholzer et al. [16], mean power during the 40-min time trial was $223 \pm 39\,W$ at $300\,m$ and $199 \pm 34\,W$ at $2800\,m$ [29]. Because P_0 is defined in the present model at $h = 0$, the $300\,m$ value was converted to its sea level equivalent value using the normalized MacInnis factor. For $V_0 = 60\,mL \cdot kg^{-1} \cdot min^{-1}$, Equation (26) gives, $F_{MI}\,(300\,m, 60) = 0.9851$. Thus

$$P_0\,(40\,min) = \frac{223\,W}{F_{MI}\,(300\,m, 60)} = \frac{223\,W}{0.9851} \simeq 226.4\,W$$

Accordingly, $P_0 = 226\,W$ was used as the primary reference value. To assess the influence of baseline sustainable power on the predicted optimum, additional calculations were performed over an approximate range of $190 - 265\,W$, corresponding to the experimental dispersion reported for the same reference population [16, 19, 20].

Road gradient was treated as a controlled model parameter rather than as a universal empirical constant. Following the mechanical formulation validated by Martin et al. [1], the road gradient was defined as $G = \tan\theta$. A 6% gradient was selected as the primary climbing scenario, while $G = 0, 3\%$, and 9% were additionally evaluated to determine how the balance between aerodynamic benefit and gravitational demand changes from level cycling to progressively steeper climbing conditions. These gradient values are prescribed numerical scenarios and are not intended to represent population-average road gradients.

For the NRLMSIS 2.0 calculations, the atmospheric forcing state was held fixed during each latitude-sensitivity experiment. Specifically, geographic longitude, date, universal time, daily $F_{10.7}$, the centered 81-day mean $F_{10.7A}$, and the geomagnetic activity input A_p were kept identical while geodetic latitude was varied. This procedure isolates the latitude dependence of the coupled atmospheric–mechanical model from temporal and space-weather variability [3]. The exact NRLMSIS input values used in the numerical calculations are reported in Table I to ensure full reproducibility. An additional controlled sensitivity analysis was performed to quantify the seasonal contribution to atmospheric density. Representative dates near the March equinox, June solstice, September equinox, and December solstice were evaluated at fixed latitude, longitude, universal time, $F_{10.7}$, $F_{10.7A}$, and A_p. Holding solar and geomagnetic forcing constant isolates the seasonal component of the NRLMSIS formulation from contemporaneous space-weather variability.

Parameter	Primary value	Atmospheric case	Date
Altitude range	$0 - 4000\,m$	March equinox	20 March 2026
Altitude increment	$10\,m$	June solstice	21 June 2026
Geodetic latitudes	$0°, 45°, 71°$	September equinox	22 September 2026
Geographic longitude	$-74°$	December solstice	21 December 2026
Primary date	10 August 2026		
Universal Time	12:00 UTC		
$F_{10.7}$	$93.7\,sfu$		
$F_{10.7A}$	$115.3\,sfu$		
A_p	$[3, 2, 5, 5, 3, 5.75, 28.875]$		

TABLE I. Atmospheric inputs prescribed for the NRLMSIS 2.0 calculations. Solar and geomagnetic forcing were held fixed during the latitude- and day-of-year sensitivity analyses to isolate the corresponding atmospheric dependencies.

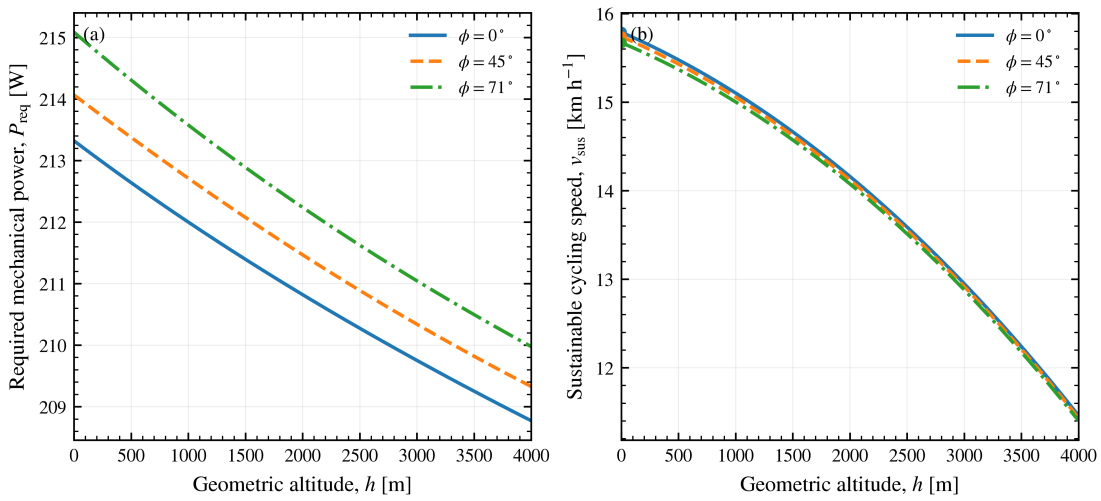


FIG. 3. Mechanical and coupled cycling responses to geometric altitude for the three latitude cases considered. (a) Required mechanical power P_{req} at a prescribed cycling speed of $15\,km \cdot h^{-1}$ and a road gradient of 6%. The decrease in P_{req} with altitude confirms the reduction in mechanical demand predicted by the model. (b) Sustainable cycling speed v_{sus} obtained from the equality between required and physiologically available mechanical power for the same 6% climbing condition. The primary calculation uses $V_0 = 60\,mL \cdot kg^{-1} \cdot min^{-1}$, $P_0 = 226\,W$, $C_dA = 0.30\,m^2$, $c_r = 0.0032$, and $m_s = 78\,kg$.

Figure 3(a) confirms that the required mechanical power at fixed speed decreases monotonically with altitude at all three latitudes. The higher required power at increasing latitude is primarily associated with the corresponding increase in normal gravity. However, the coupled response shown in Fig. 3(b) demonstrates that this mechanical benefit does not compensate for the physiological loss during the reference 6% climb. Sustainable speed decreases continuously with altitude, and no interior optimum is found over the $0 - 4000\,m$ interval. The constrained optimum therefore occurs at the lower boundary.

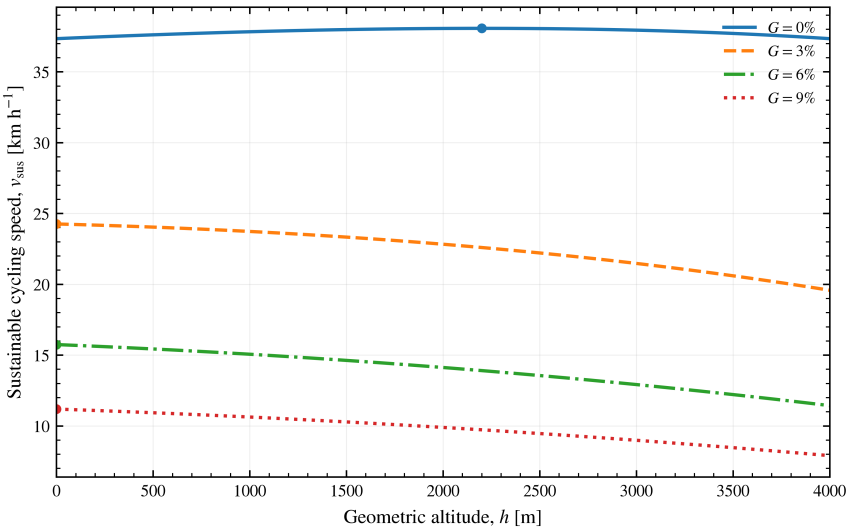


FIG. 4. Sensitivity of sustainable cycling speed to road gradient at $\phi = 45°$. Curves correspond to $G = 0, 3, 6$, and 9%, while atmospheric, physiological, aerodynamic, and cyclist–bicycle parameters are held at their reference values. Markers identify the constrained optimum within the $0 - 4000\,m$ interval. An interior altitude optimum appears under level-cycling conditions, whereas positive gradients progressively shift the model toward physiologically and gravitationally dominated behavior.

Figure 4 demonstrates that the existence of an optimal cycling altitude is strongly dependent on road gradient. Under level-cycling conditions, sustainable speed initially increases with altitude and reaches an interior maximum near $2.2\,km$ before decreasing. In contrast, for the $3, 6$, and 9% gradients considered here, sustainable speed decreases from sea level. Consequently, the optimal altitude is not a universal environmental quantity but an emergent property of the balance among aerodynamic resistance, gravitational demand, and altitude-induced physiological impairment.

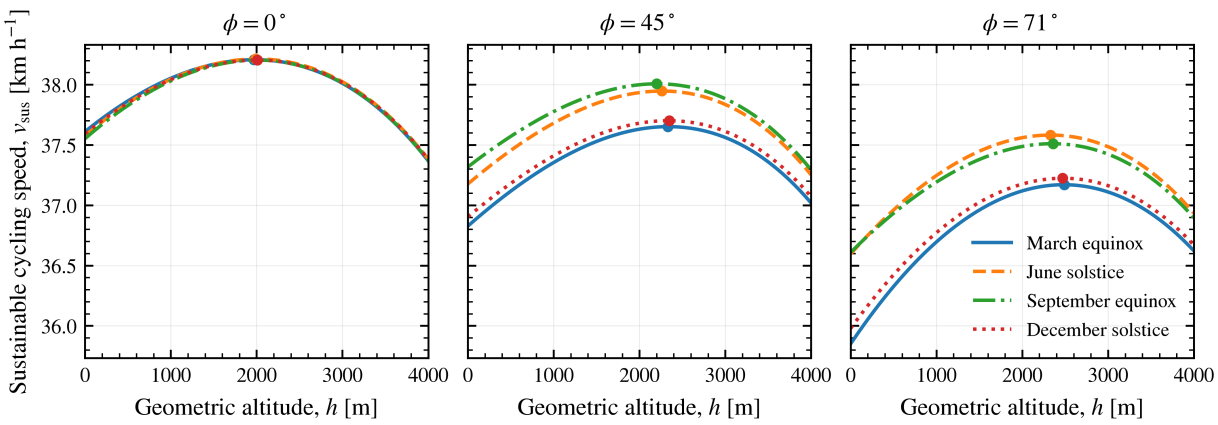


FIG. 5. Latitude dependence of the seasonal sensitivity of sustainable cycling speed under level-cycling conditions. Seasonal $v_{sus}\,(h)$ profiles are shown for (a) $\phi = 0°$, (b) $\phi = 45°$, and (c) $\phi = 71°$, using representative dates near the March equinox, June solstice, September equinox, and December solstice. Longitude, Universal Time, daily $F_{10.7}$, the centered 81-day mean $F_{10.7A}$, geomagnetic activity, and all cyclist and bicycle parameters were held fixed. Markers indicate the interior maximum of each seasonal curve. Seasonal differences are minimal at the Equator but become progressively more pronounced at mid and high latitudes, demonstrating a coupled latitude-day-of-year dependence of the modeled performance optimum.

Figure 5 reveals a marked latitude dependence of the seasonal atmospheric effect on sustainable cycling performance. Under level-cycling conditions, all combinations of latitude and season exhibit an interior maximum in $v_{sus}\,(h)$, but both its magnitude and location depend on the prescribed atmospheric state. At the Equator, the four seasonal profiles are nearly coincident, with maximum sustainable speeds close to $38\,km \cdot h^{-1}$ and optimal altitudes near $2.0\,km$. At $\phi = 45°$, seasonal differences become appreciable, with the maximum occurring at approximately $2.2 - 2.4\,km$ and the seasonal spread in maximum speed approaching $0.35\,km \cdot h^{-1}$. At $\phi = 71°$, the seasonal modulation remains pronounced, with optimal altitudes of approximately $2.3 - 2.5\,km$ and differences in maximum sustainable speed of the order of $0.4\,km \cdot h^{-1}$. Because cyclist, bicycle, physiological, solar, and geomagnetic parameters are held fixed among the seasonal cases at each latitude, the separation between seasonal curves arises from the day-of-year dependence of the NRLMSIS 2.0 atmospheric density field.

V. DISCUSSION

The present results show that the mechanical benefit of altitude cannot be interpreted independently of road gradient and physiological impairment. At a prescribed cycling speed, both decreasing atmospheric density and the small altitude-induced reduction in normal gravity lower the required mechanical power. However, once sustainable speed is determined from the equality between required and physiologically available power, the resulting performance response depends strongly on the relative contribution of aerodynamic and gravitational resistance.

This distinction explains the different behavior predicted for level cycling and sustained climbing. Under level conditions, aerodynamic drag represents the dominant external resistance at competitive cycling speeds, allowing the reduction in atmospheric density to offset the physiological penalty over an initial altitude range. An interior optimum therefore emerges. As road gradient increases, the gravitational term becomes progressively more important while the aerodynamic contribution decreases in relative importance. For the reference 6% climb, the physiological loss dominates throughout the modeled altitude range and no interior optimum is obtained.

This result also provides a useful context for comparison with hour-record studies. The altitude benefit considered by Bassett et al. [27], Harnish et al. [21], and Vinetti [26] primarily concerns level, aerodynamically dominated cycling and should therefore not be extrapolated directly to sustained climbing. The present framework reconciles these apparently different behaviors by showing that the existence of an altitude optimum depends on the mechanical regime rather than on altitude alone.

The NRLMSIS 2.0 calculations further indicate that the atmospheric contribution depends jointly on latitude and day of year. Seasonal differences are minimal under the equatorial conditions considered here but become progressively more pronounced at mid and high latitudes. This interaction cannot be reproduced by an altitude-only standard atmosphere and illustrates the value of explicitly retaining geographic and temporal atmospheric dependence when small performance differences are relevant.

Several limitations should nevertheless be considered. The MacInnis meta-regression describes acute hypoxic exposure and does not explicitly model acclimatization. In addition, Equation (23) assumes that the relative reduction in sustainable mechanical-power availabil-

ity scales with the relative reduction in $\dot{V}O_{2\,\max}$; this is a modeling approximation rather than a physiological identity. Wind, changes in cyclist posture, drivetrain losses, transient gradients, and route-specific meteorological conditions are also excluded. The present formulation should therefore be interpreted as a controlled theoretical framework rather than as a route-specific performance predictor.

Furthermore, the physiological scaling is parameterized directly in terms of geometric altitude and does not incorporate latitude- or day-of-year-dependent variations in local barometric pressure. Consequently, the geographic and seasonal NRLMSIS effects enter the present coupled model primarily through the aerodynamic pathway.

VI. CONCLUSIONS

The present study develops a coupled geodetic–atmospheric–physiological framework for sustainable cycling performance at altitude. The formulation explicitly separates the mechanical power required by the cyclist–bicycle system from the physiologically available mechanical power, combining WGS84 normal gravity, NRLMSIS 2.0 atmospheric density, and the corrected MacInnis altitude-response model.

The calculations confirm that the mechanical power required to maintain a prescribed cycling speed decreases with altitude. However, this mechanical benefit does not necessarily improve performance. Under the reference 6% climbing condition, altitude-induced physiological impairment dominates the reduction in mechanical demand and sustainable speed decreases monotonically over $0 - 4000\,m$. Consequently, no interior critical altitude exists and the constrained optimum occurs at the lower boundary.

In contrast, level cycling produces an interior optimum at approximately $2.0 - 2.5\,km$, depending on latitude and atmospheric state. Increasing road gradient suppresses this altitude advantage, demonstrating that the optimum emerges from the balance among aerodynamic resistance, gravitational demand, and physiological impairment.

Controlled NRLMSIS 2.0 calculations further reveal a latitude-dependent day-of-year effect. Seasonal differences are minimal at the Equator but become appreciable at mid and high latitudes, approaching 1% in maximum sustainable speed. Thus, latitude and day-of-year effects cannot generally be represented as independent additive corrections to a standard atmosphere.

Optimal cycling altitude should therefore be regarded as a multivariable quantity rather than as a universal elevation. An interior critical altitude h_c exists only when the mechanical benefit of increasing altitude initially exceeds the corresponding physiological penalty. This framework reconciles the potential advantage of altitude under level, aerodynamically dominated conditions with the progressively greater physiological disadvantage associated with sustained climbing.

ACKNOWLEDGMENTS

Fruitful discussions with Diego Pacheco are gratefully acknowledged.

---

[1] Martin JC, Milliken DL, Cobb JE, McFadden KL, Coggan AR. (1998). Validation of a mathematical model for road cycling power. Journal of Applied Biomechanics, 14(3), 276–291.

[2] Department of Defense World Geodetic System 1984 — Its Definition and Relationships with Local Geodetic Systems, Version 1.0.0, NGA.STND.0036_1.0.0_WGS84.

[3] Emmert JT, Drob DP, Picone JM, Siskind DE, Jones M, et al. NRLMSIS 2.0: A Whole-Atmosphere Empirical Model of Temperature and Neutral Species Densities. Earth and Space Science. 2021;8:e2020EA001321. doi:10.1029/2020EA001321.

[4] Moritz, H. (2000). Geodetic Reference System 1980. Journal of Geodesy, 74(1), 128-133.

[5] U.S. Standard Atmosphere, 1976. NOAA, NASA, U.S. Air Force. U.S. Government Printing Office, Washington, DC, 1976.

[6] Heiskanen, W. A., & Moritz, H. , Physical Geodesy (1967). W.H. Freeman and Company.

[7] Torge, Geodesy, 3rd edition, 2001, De Gruyter.

[8] Wehrlin JP, Hallén J. Linear decrease in $\dot{V}O_{2\,\max}$ and performance with increasing altitude in endurance athletes. European Journal of Applied Physiology. 2006;96(4):404–412. doi: 10.1007/s00421-005-0081-9. Epub 2005 Nov 26. PMID: 16311764.

[9] Hahn AG, Gore CJ. The effect of altitude on cycling performance: a challenge to traditional concepts. Sports Medicine. 2001;31(7):533–557. doi: 10.2165/00007256-200131070-00008. PMID: 11428690.

[10] Calbet JA, Boushel R, Radegran G, Søndergaard H, Wagner PD, Saltin B. (2003). Why is

$VO_{2\,\max}$ after altitude acclimatization still reduced despite normalization of arterial O_2 content?. American Journal of Physiology-Regulatory, Integrative and Comparative Physiology. 2003;284(2):R304–R316. doi: 10.1152/ajpregu.00156.2002. Epub 2002 Oct 3. PMID: 12388462.

[11] Garvican-Lewis LA, Clark B, Martin DT, et al. Impact of altitude on power output during cycling stage racing. PLoS ONE. 2015;10(12):e0143028. doi:10.1371/journal.pone.0143028.

[12] Van Erck, D., Wenker, E. J., Levels, K., Foster, C., de Koning, J. J., & Noordhof, D. A. (2019). Cycling at Altitude: Lower Absolute Power Output as the Main Cause of Lower Gross Efficiency. International Journal of Sports Physiology and Performance, 14(8), 1117–1123. doi:10.1123/ijspp.2018-0221.

[13] Townsend NE, Nichols DS, Skiba PF, Racinais S, Périard JD. Prediction of Critical Power and W' in Hypoxia: Application to Work-Balance Modelling. Front Physiol. 2017 Mar 23;8:180. doi: 10.3389/fphys.2017.00180. PMID: 28386237; PMCID: PMC5362642.

[14] Hawley JA, Noakes TD. Peak power output predicts maximal oxygen uptake and performance time in trained cyclists. Eur J Appl Physiol Occup Physiol. 1992;65(1):79-83. doi: 10.1007/BF01466278. PMID: 1505544.

[15] Wagner PD. The physiological basis of reduced $VO_{2\,\max}$ in Operation Everest II. High Altitude Medicine & Biology. 2010;11(3):209-215. doi:10.1089/ham.2009.1058.

[16] Oberholzer L, Aamaas NS, Hallén J. Changes in cycling economy and fractional utilization of $\dot{V}O_{2peak}$ during a 40-min maximal effort exercise test with acute hypobaric hypoxia corresponding to 2800 m of altitude. Scandinavian Journal of Medicine & Science in Sports. 2024;34(1):e14511. doi:10.1111/sms.14511.

[17] Péronnet F, Bouissou P, Perrault H, Ricci J. (1989). Comparaison du record de l'heure cycliste selon l'altitude et le matériel utilisé. Canadian Journal of Sport Sciences, 14(2), 93–98. French. PMID: 2736448.

[18] Péronnet F, Thibault G, Cousineau DL. A theoretical analysis of the effect of altitude on running performance. Journal of Applied Physiology, 70(1), 399–404. doi: 10.1152/jappl.1991.70.1.399. PMID: 2010398.

[19] MacInnis MJ, Nugent SF, MacLeod KE, Lohse KR. (2015). Methods to Estimate $\dot{V}O_{2,\max}$ upon Acute Hypoxia Exposure. Medicine & Science in Sports & Exercise, 47(9), 1869–1876. doi:10.1249/MSS.0000000000000628. PMID 25668403.

[20] Methods to Estimate $\dot{V}O_{2,\max}$ upon Acute Hypoxia Exposure—Corrigendum. Medicine &

Science in Sports & Exercise. 2018;50(12):2618. doi:10.1249/MSS.0000000000001807. PMID: 30431547.

[21] Harnish CR, Swinand GP, Fisher AE. Making History in 1 h: How Sex, Aging, Technology, and Elevation Affect the Cycling Hour Record. Medicine & Science in Sports & Exercise. 2024;56(3):454–463. doi:10.1249/MSS.0000000000003328. PMID: 38051143.

[22] Deb SK, Brown DR, Gough LA, McLellan CP, Swinton PA, Sparks SA, McNaughton LR. Quantifying the effects of acute hypoxic exposure on exercise performance and capacity: A systematic review and meta-regression. European Journal of Sport Science. 2018;18(2):243–256. doi:10.1080/17461391.2017.1410233. PMID: 29220311.

[23] West, J. B., & Luks, A. M. (2021). Respiratory system under stress. In West's respiratory physiology: The essentials (11th ed., pp. 172–194). Wolters Kluwer.

[24] Debraux P, Grappe F, Manolova AV, Bertucci W. (2011). Aerodynamic drag in cycling: methods of assessment. Sports Biomechanics, 10(3), 197–218. doi:10.1080/14763141.2011.592209. PMID 21936289.

[25] Crouch TN, Burton D, LaBry ZA, Blair KB. Riding against the wind: a review of competition cycling aerodynamics. Sports Engineering. 2017;20(2):81–110. doi:10.1007/s12283-017-0234-1.

[26] Vinetti G. (2025). Breaking the Cycling Hour Record: Is There Still Room for Altitude? Medicine & Science in Sports & Exercise, 57(8), 1825–1826. DOI: 10.1249/MSS.0000000000003710. PMID: 40289781.

[27] Bassett DR Jr, Kyle CR, Passfield L, Broker JP, Burke ER. Comparing cycling world hour records, 1967–1996: modeling with empirical data. Medicine & Science in Sports & Exercise. 1999;31(11):1665–1676. doi:10.1097/00005768-199911000-00025.

[28] Howley ET. Effect of altitude on physical performance. In: Stull GA, Cureton TK, eds. Encyclopedia of Physical Education, Fitness, and Sports: Training, Environment, Nutrition, and Fitness. 1980;177–187.

[29] Oberholzer L, Aamaas NS, Hallén J. The fractional utilization of $\dot{V}O_{2,\max}$ is higher in hypobaric hypoxia equivalent to $2800m$ than near sea level. In: 27th Annual Congress of the European College of Sport Science, Sevilla, Spain, 30 August–2 September 2022. Book of Abstracts; 2022:90.